



Evolution of events before and after the 17 June 2017 landslide at Karrat, West Greenland – a multidisciplinary approach for studying landslides in a remote arctic area

5 Kristian Svennevig¹, Trine Dahl-Jensen¹, Marie Keiding¹, John Peter Merryman Boncori², Tine B. Larsen¹, Sara Salehi¹, Anne Munck Solgaard¹ and Peter H. Voss¹

¹Geological Survey of Denmark and Greenland (GEUS), Copenhagen, 1350, Denmark.

²DTU Space, National Space Institute, Technical University of Denmark, Lyngby, 2800, Denmark.

10 *Correspondence to:* Kristian Svennevig (ksv@geus.dk)

Abstract. The 17 June 2017 rock avalanche on the south facing slope of the Ummiammakku Mountain (Karrat Isfjord, West Greenland) caused a tsunami that flooded the nearby village of Nuugaatsiaq, killed four persons and destroyed 11 buildings. Landslide activity in the area was not previously known and the disaster gave rise to important questions about what events led up to the landslide and what the future hazard is in the area around the landslide? However, the remoteness of the area and difficult fieldwork conditions, made it challenging to answer these questions. We apply a multidisciplinary workflow to reconstruct a timeline of events on the coastal slope here collectively termed the Karrat Landslide Complex. The workflow combines limited fieldwork with analyses of freely available remote sensed data comprising seismological records, Sentinel-1 space borne Synthetic Aperture Radar (SAR) data and Landsat and Sentinel-2 multispectral optical satellite imagery.

Our analyses show that at least three historic rock avalanches occurred in the Karrat Landslide Complex: Karrat 2009, Karrat 2016 and Karrat 2017. The last is the source of the tsunami and the first two are described for the first time here. All three are interpreted to have initiated as translational rockslides. In addition to the historical rock avalanches, several pre historic rock avalanche deposits are observed, demonstrating older periods of activity. Furthermore, three larger areas of continuous activity are described and may pose a potential future hazard. A number of non-tectonic seismic events confined to the landslide complex are interpreted to record landslide activity. Based on the temporal distribution of events in the landslide complex, we speculate that the possible trigger for landslides is permafrost degradation caused by climate warming.

The results of the present work highlight the benefits of a multidisciplinary approach based on freely available data to studying landslides in remote Arctic areas under difficult logistical field conditions and demonstrates the importance of identifying minor precursor events to identify areas of future hazard.



Introduction

On 17 June 2017 the village of Nuugaatsiaq in West Greenland was hit by a tsunami generated by a 35-58 million m³ landslide on the south facing slope of the Ummiammakku mountain in Karrat Isfjord located 32 km to the east of the village (Bessette-Kirton et al., 2017; Clinton et al., 2017; Gauthier et al., 2018; Paris et al., 2019). A large part of the village was destroyed, and four people lost their lives. The tsunami was also observed in other settlements more than 100 km away. Following this, the Greenlandic authorities evacuated 170 residents from Nuugaatsiaq and the neighbouring settlement of Illorsuit due to the threat of further landslides in the area and the villages continue to be evacuated at the time of this writing due to fear of additional landslide triggered tsunamis (Fig. 1). The Karrat Landslide highlights the necessity to screen the inhabited parts of Greenland for unstable slopes and to map previous large landslides to assess the risk of future tsunamigenic events.

Fieldwork and in situ measurements are difficult and time consuming in a vast and remote Arctic environment like Greenland where infrastructure is minimal and expensive. Thus, investigations of unstable slopes over large parts of Greenland must primarily rely on remote sensing techniques. Following the launch of Landsat-8 and Sentinel-1 and 2 satellites, optical and SAR data over Greenland is both free and frequent and at sufficient resolution, providing a means of observing deforming slopes at relatively low cost. Svennevig et al. (2019) developed a multi-disciplinary approach combining satellite SAR, optical data, and seismic observations to study remotely activity on an unstable slope. They found that by combining these methods it was possible to reliably detect timing (seismic observations), location, extent and deformational rates (optical images, deformation from DInSAR (Differential Interferometric Synthetic Aperture Radar) of landslide activity.

Our aims with this study are twofold: to understand the processes that led to the catastrophic Karrat 2017 rock avalanche, and to evaluate the risk of further landslides at Ummiammakku Mountain. Following the multi-disciplinary approach of Svennevig et al. (2019) it is possible to resolve the series of events leading up to and following the disaster in Karrat Fjord in June 2017. We show that it would not be possible to establish both timing and location of all events based on one method alone. We contextualize our results using geological knowledge of the area derived from limited fieldwork and previous studies and discuss the possible landslide trigger mechanism.

Geological Setting and Background of the study site

The geology of the Karrat region is dominated by Archean gneiss interfolded with supracrustal rocks of the Palaeoproterozoic Karrat Group (Henderson and Pulvertaft, 1967; Sørensen and Guarnieri, 2018) (Fig. 1B). Locally around the Karrat 2017 rock avalanche, the succession consists of the Archean Umanak gneiss overlain by Palaeoproterozoic Quartzite and semipelitic to pelitic schist of the Karrat Group (Mott et al., 2013). The slopes in the region are permafrozen (Westergaard-Nielsen et al., 2018).

No previous historic landslides are described from the coast under Ummiammakku in the Karrat Fjord area but two tsunami-generating landslides in 1952 and 2000 are described from Vaigat 150 km to the south of Karrat (Dahl-Jensen et al., 2004; Pedersen et al., 2002). Svennevig (2019) described several Holocene landslides in the region but noted that the majority of these were focused to the area of the Cretaceous-Paleogene Nuussuaq Basin, where the 1952 and 2000



landslides also occurred. The geologic province where the 2017 landslide occurred was found to have relatively few
landslides (Fig. 1a). Field observations show that the Palaeoproterozoic rocks on the slope parts easily along distinct
70 layering of the bedding (s0 foliation) which dips 20 to 30° to the south towards the fjord. Furthermore, E-W orientated
vertical penetrative open fractures with a normal offset are observed locally on the slope (Fig. 2F).

Methods and data

We use a workflow integrating seismological data, SAR and optical imagery – all publicly available – for describing the
75 evolution of the Karrat Landslide Complex. These data sources have different temporal and spatial resolution ranging
from years to milliseconds and meters to 10's of kilometres (see table 1). Individually they have unique information for
studying landslides, but tell an incomplete story by themselves and the value of the individual datasets increases
significantly when integrated. The workflow is described and applied in Svennevig et al. (2019) examining a minor (ML
1.9) non tectonic seismic event in the Karrat Landslide Complex on 26 March 2018.

80 We found that alerting each other across disciplines of suspected smaller landslide events enabled us to construct a reliable
multi-year sequence of both confirmed smaller landslides and periods of activity in the area. For example, if a seismic
event was suspected of being caused by a landslide, optical satellite images before and after the time of the seismic event
was inspected for changes, and InSAR (Interferometric Synthetic Aperture Radar) images constructed for evidence of
movement. Alternatively, if optical satellite images showed change between two satellite passages, we could check if a
85 seismic event had occurred in the area in the time interval, and if InSAR analyses showed movement to confirm either
minor activity or indeed a landslide.

Fieldwork

Because of the remoteness of the area and the steepness of the coastal slope carrying out fieldwork is logistically
90 challenging. Because of the continued risk of landslides (see below) and near constant minor rockfalls (Fig. 2E) it is not
safe to come closer than about 1.5 km of the landslide area. These conditions highlight the need for remotely sensed data
as exemplified below. We visited areas just east and west of the Karrat 2017 rock avalanche on two short reconnaissance
stops during the summer of 2019 to make observations of the surrounding geology and to inspect the landslide area using
a camera-equipped multirotor UAV (Unmanned Aerial Vehicle).

95

DInSAR

Slope deformation can be detected remotely using DInSAR-based techniques (Carlà et al., 2019; Rosen et al., 2000),
which provide one-dimensional ground-motion measurements between two radar acquisitions in a radar equipped satellite
line-of-sight direction, i.e. towards and away from the radar. The Sentinel-1A and -1B are Earth monitoring synthetic
100 aperture radar (SAR) satellites operated by the European Space Agency (ESA) that covers all of Earth's landmass. The
data produced from these platforms is freely available distributed by the ESA. The Sentinel-1 data acquired over land
provide 5 m x 20 m spatial resolution in the ground range and azimuth (flight-path) directions respectively. Two satellite



tracks cover the Karrat area during the period of interest: ascending track 90 (available from October 2014) and descending track 25 (available from July 2017). The viewing geometry of track 25 is best suited for detecting movements
105 on the slopes in our region of interest. Unfortunately, large parts of the steep slopes that failed in 2016 and 2017 cannot be observed with the viewing geometry of ascending track 90 that covers the pre-failure time period. SAR data is insensitive to cloud cover and the polar night as opposed to optical satellite data from e.g. Sentinel-2 (see below). However, a prerequisite for the applicability of DInSAR is a sufficient level of statistical similarity (interferometric coherence) between the electromagnetic properties of the surface at the two acquisition times. This can be lost due to
110 changes in the satellite viewing geometry or physical changes at the surface between acquisitions. Ground motion of more than half a wavelength (2.8 cm for Sentinel-1) between acquisitions will cause a complete loss of coherence, called decorrelation, in the image. In practise, decorrelation occurs at lower ground motion due to the other factors affecting the coherence. Sentinel-1 data are acquired every 6 days over Greenland, and for this study both 6 and 12 days differential interferograms were used. The topographic contribution to the interferometric phase was removed using ArcticDEM
115 version 2.0 (Porter et al., 2018). For interferograms following the June 2017 landslide, the ArcticDEM was locally corrected with a DEM (digital elevation Model) derived from oblique photogrammetry collected in the summer of 2017 (courtesy of E.V. Sørensen, GEUS).

Seismology

120 The Geological Survey of Denmark and Greenland (GEUS) monitors seismic activity in Greenland using the Greenland Ice Sheet Monitoring Network (GLISN network, www.glisn.info), which consists of 21 stations (Clinton et al., 2014). Detecting and accurately locating the activity in the Karrat area depends on having a sufficient number of nearby stations (see Fig. 1A). The stations in this area are located along the coast with a distance of at least 100 km between them. Thus, the horizontal location uncertainty of detected earthquakes or other types of seismic events is up to 50 km, in particular
125 in the east-west direction.

Not only tectonic earthquakes are detected in Greenland. We see many events that we classify as non-tectonic events. This class of events were first described by Ekström et al. (2003) and were found to be located at Greenland's large outlet glaciers. The monitoring carried out by GEUS locate many non-tectonic events smaller than the globally detected events described by (Ekström et al. (2003), and also many of these are located close to large outlet glaciers. The causes of non-
130 tectonic events are several. For example, events with epicentre located near an outlet glacier (cryo-seismic events) often contain a low frequency component, and are usually much longer in duration than tectonic earthquakes (Fig. 5), and are interpreted to be caused by calving of glaciers (Ekström et al., 2003; Nettles et al., 2008). Other non-tectonic events, in Western Greenland, are mainly caused by sea ice breakup, glacier or sea ice movements on bedrock, but other types are also present see e.g. Podolskiy and Walter (2016). Suddenly failing landslides also produce a seismic signal. The Karrat
135 2017 rock avalanche was seen globally as a Ms 4.2 event (U.S. Geological Survey, 2020), and the 2000 Paatut landslide was seen throughout Greenland (Dahl-Jensen et al., 2004). Smaller events associated with known landslides (this paper) are only seen more locally (Fig. 5).

Non-tectonic events can easily be identified from tectonic earthquakes based on their different frequency content and P and S amplitudes (Fig. 5).



140 However, distinguishing a landslide signal from other non-tectonic events, such as events associated with glaciers, is not straightforward. The seismic signature from two very large landslide events, the 2000 Paatuut landslide (Dahl-Jensen et al., 2004) and the 2017 Karrat rock avalanche have long lasting tremor signals and a strong low frequency component. For smaller landslides the tremor component will be smaller in duration and amplitude. Many aspects of smaller known landslide events are similar to cryo-seismic events (Fig. 5). There are several large outlet glaciers in the Karrat area
145 responsible for non-tectonic events within the horizontal uncertainty of the location of events, so the location in itself is not sufficient to distinguish whether the source is a glacier outlet or possibly a landslide. In the Discussion section of this paper a first step towards distinguishing between these two types on non-tectonic events is described.

Seismological data enabling us to register and locate smaller non-tectonic events became available around 2008. The first station in Greenland was in operation 1906-1912. In the late 1920's two more permanent stations were installed. Until
150 the 1990's the network consisted of only 3-4 stations, increasing to 5-8 stations around 2000. The present GLISN network was rolled out from 2008 to 2010 and has 21 operational stations. Before 2010 only very large landslides would have been observed on the seismic stations, for example the Paatuut 2000 landslide (Dahl-Jensen et al., 2004), which by luck also coincided with a research network station deployment (Dahl-Jensen et al., 2003).

155 ArcticDEM

ArcticDEM is a freely available 2 m spatial resolution digital elevation model (DEM) covering all of the arctic area north of 60°N (Porter et al., 2018). As such, it has the highest spatial resolution of publicly available datasets covering Greenland. The DEM is derived from high-resolution (~0.5 m pixel size) stereo satellite imagery from the commercial WorldView satellites. The source images are not publicly available. Several DEM strips reflecting various image
160 acquisition times are available covering the same areas making it possible to follow the temporal evolution of landslides. For the Karrat landslide area DEM strips are available from 3 June 2008 to 23 June 2017 but in a variable quality and coverage. The area of the Karrat 2017 rock avalanche is for example only partially covered by a single ArcticDEM strip from after the landslide acquired on 23 June 2017.

165 Space borne optical (Sentinel-2)

The Sentinel-2A and -2B are Earth monitoring multispectral optical satellite imaging systems operated by ESA. They record in 13 spectral bands at various resolution: four bands at 10 m (including visual light), six bands at 20 m and three bands at 60 m spatial resolution as such they are currently the highest resolution freely available optical data sets covering Greenland. Sentinel-2A was launched in June 2015 and Sentinel-2B was launched in March 2017. Revisiting time is
170 every five days at the equator but at higher latitudes such as Greenland most areas are covered twice or more every five days. At high latitudes with constant winter darkness there is a data gap in the winter months. For this reason, there is a yearly data gap at the Karrat Landslide Complex from the end of October to start of March. For the present study, we have only performed visual interpretation of the Sentinel-2 images. Data are freely available from ESA.



175 Space borne optical (Landsat)

The Landsat program is a series of Earth monitoring multispectral optical satellites, the first of which, was launched in 1972. Landsat 1-5 (1972-1993) had spatial resolutions of 60 m and Landsat 6-8, a 30 m resolution. Landsat-7 and -8 revisits the same area every eight day since the launch of Landsat-8 in 2013. Further back in time the coverage is sparser. As is the case for Sentinel-2 scenes Landsat images at this high latitude have a winter data gap from mid-October to start-

180 March. Data are freely available from USGS within 24 hours of acquisition.

Aerial images

To constrain the evolution of the Karrat Landslide Complex a set of 1:45 000 scale black and white aerial images from 1953 (available from The Danish Agency for Data Supply and Efficiency) have been analysed. These constitutes the

185 oldest known aerial images from the area.

Table 1: Temporal and spatial resolution of the various datasets.

Method/source		Resolution		Period
		Spatial	Temporal	
<i>Space borne InSAR (Sentinel-1)</i>		5x20 m	6 days	Since 2014
<i>Seismology</i>		10 to 100s of km	seconds	since ~2000
<i>ArcticDEM</i>		2 m	years/months	Variable from 2008 to 2017
<i>Optical</i>	<i>Space borne (Sentinel-2)</i>	10 m	Few days	since 2015
	<i>Space borne (Landsat)</i>	30-60 m	Weeks - Months	Since 1973
	<i>Aerial images nadir</i>	20-30 m	years/decades	Variable since 1953

Results – landslides and active areas at the Karrat Landslide Complex

In order to describe the multifaceted landslide evolution of the Karrat area it is necessary to establish a nomenclature

190 framework. Hence, we introduce the Karrat Landslide Complex as a 3 by 9 km area of past, present and future landslide activity on the south facing slope of Karrat Isfjord 30 km east of Nuugaatsiaq, West Greenland (Fig. 1A). Landslides in the Karrat Landslide Complex are named Karrat followed by the year they happened and type of landslide e.g. Karrat 2017 rock avalanche. Larger areas experiencing downslope creep that have not yet failed catastrophically yet are termed unstable areas 1, 2 and 3 respectively with Area one being the oldest and Area 3 the youngest (Fig. 1B). Numerous shallow

195 non-tectonic seismic events that are not associated with catastrophic landslides, are named after the date they happened and seismic event, e.g. 2017-06-01 seismic event. These events are suggested to be related to activity in the Karrat Landslide Complex. Confirmed landslides, active areas and other activity which are interpreted to possibly be landslides



are described below, and are listed chronologically from oldest to newest in table 2, bearing in mind that the list is probably not complete.

200

The confirmed landslides

The Karrat 2009 rock avalanche ($71^{\circ}38'20''\text{N}$, $52^{\circ}19'16''\text{W}$, 1 September 2009 at 14:09Z, ML 2.7)

205 The scar of the 2009 rock avalanche shows that it released along a near-vertical back scarp and a basal sliding plane defined by bedding dipping $10\text{--}30^{\circ}$ toward the fjord (Fig. 3B). Based on this, we suggest that the 2009 avalanche initiated as a translational landslide and developed into a rock avalanche. The timing of the avalanche was initially confined to a five year interval by the two oldest ArcticDEM strips (3 June 2008 – 12 October 2013). It was then further confined to an eight-day interval between 26 August and 2 September in 2009 by visual inspection of Landsat 7 scenes. The area appears as a 0.4 km^2 dark coloured patch in the latter scene. The interpretation of this patch as a landslide was confirmed by inspection of the following ArcticDEM scene from 12 October 2013 and a Sentinel-2 scene from 30 July 2016. A screening of the seismicity for the period 26 August 2009 to 2 September 2009 revealed a likely candidate on 1 September 210 2009 at 14:09Z as an ML 2.7 magnitude seismic event located within a 60 by 6 km EW oriented ellipsoid. The landslide was previously termed The East landslide by Bessette-Kirton et al. (2017) and was suggested to occur between 23 May 2009 and 28 April 2011 based on interpretation of Worldview images. Based on ArcticDEM strips from before (3 June 2008) and after the landslide we calculate the volume of the scarp to be $2.7 \times 10^6\text{ m}^3$ and the lobe to be $2.8 \times 10^6\text{ m}^3$. That 215 these volumes are roughly the same indicates that none of the material reached the sea and the Karrat 2009 rock avalanche is thus unlikely to have produced a tsunami. InSAR data from 2015 show that the depositional lobe was not completely stable six years after the avalanche.

The Karrat 2016 rock avalanche ($71^{\circ}38'24''\text{N}$, $52^{\circ}19'41''\text{W}$, 15 November 2016 at 14:09Z, ML 2.1)

220 The 2016 Karrat avalanche occurred immediately west of the 2009 scar, and its structural situation is the same (Fig. 1B, 3C). Both avalanches occurred along the same c. east-west oriented vertical surface as back scarp and c. 20° dip slope weakness as basal sliding plane. Based on Sentinel-2 images, the Karrat 2016 rock avalanche occurred between 12 October 2016 and 1 March 2017. The large time uncertainty is because the area is in constant darkness during the winter and no optical data is thus available to pinpoint the time more accurately. However, InSAR scenes from 11 and 17 November 2016 show loss of coherence of the area indicating the most possible time interval of the avalanche (Fig. 4C). 225 Optical data is not very helpful in this case due to darkness, although it is in agreement with InSAR. Analysis of the seismic signal reveals a magnitude ML 2.1 non tectonic event to take place at 15 November 2016 at 11:34Z (Fig. 5D). The westernmost part of the slide scarp is visible in an ArcticDEM strip from 5 June 2017. Based on this DEM and the geometric constraints of the scarp of the Karrat 2009 rock avalanche we calculate the volume to be $3.0 \times 10^6\text{ m}^3$. It is not possible to constrain the volume of the deposit from the landslide as no DEM covers the entire area. However, based on 230 the Sentinel-2 images, it seems that some of the material may have reached the fjord (Fig 3C). Bessette-Kirton et al. (2017) described an enlargement of their East landslide (here named the Karrat 2009 rock avalanche) that took place sometime between 16 May 2016 and 5 June 2017, based on Worldview images. This probably corresponds to the Karrat 2016 rock avalanche.



The Karrat 2017 rock avalanche (71°38'36"N, 52°20'12"W, 17 June 2017 at 23:39Z, M_s (20 sec) 4.2)

235 The landslide of 17 June 2017 appears to be a translational landslide that developed into a rock avalanche. This is based on the same criteria as the Karrat 2009 and 2016 rock avalanches: dip slope of the bedrock on the coast and near vertical east-west oriented back scarp. The Karrat 2017 rock avalanche appears in all of our data sources, but these are secondary to the eye witness reports of the landslide and tsunami that combined with the seismic signal gives the exact timing of the event to 17 June 2017 at 23:39Z (Fig 5a). The Karrat 2017 rock avalanche is well constrained in previous preliminary

240 publications (Bessette-Kirton et al., 2017; Clinton et al., 2017; Gauthier et al., 2018). It was termed the Nuugaatsiaq landslide by Bessette-Kirton et al. (2017) and Poli (2017) after the village of Nuugaatsiaq 30 km to the West and the Greenland landslide by Chao et al. (2018). Only the easternmost part of the landslide is visible in two ArcticDEM strips covering the area from 23 and 28 June 2017. Previous volume estimates range from 35 to 76 x 10⁶ m³ (Bessette-Kirton et al., 2017; Chao et al., 2018; Gauthier et al., 2018; Paris et al., 2019) but some of these are based on DEM work that

245 does not include the full volume of the Karrat 2016 rock avalanche, see discussion. Recent work based on detailed DEMs from high resolution oblique photogrammetry from 2015 and 2017 gives a volume of 41 – 43.5 x 10⁶ m³ mobilized in the 2016 and 2017 rock avalanches (Sørensen et al in prepXX). Subtracting the volume of the Karrat 2016 rock avalanche given above gives a volume of 38–40 10⁶ m³ for the Karrat 2017 rock avalanche.

250 The active areas

Area 1 (71°38'44"N, 52°28'19"W)

Area 1 is a large well-developed active landslide 4 km west of the area of the present Karrat 2017 scar (Fig 1B) not previously described in the literature. The 2000 m by 1600 m area is defined by a well-developed up to 120 m high back scarp and lateral release surfaces. The back scarp is near the crest of a 1000 m high mountain and the unstable area extends

255 to the coast, suggesting that it continues below sea level. Internally the area shows sign of significant strain with multiple scarps, contour parallel grabens and an overall hummocky fabric (Fig. 2B). The area is well defined in the 1953 aerial images (Fig. 2A). Subareas in the lower 200 to 400 m of the slope show downslope movements between various ArcticDEM scenes. The same areas decorrelated in almost all DInSAR interferograms. Some interferograms show episodic movement of 1-5 mm/day over most of the area (Fig. 4D). Multiplying the height of the back scarp with the area

260 of the active area (120m x 2000m x 1600m) gives a tentative minimum volume of 380 x 10⁶ m³ for the area above sea level.

Area 2 (71°38'46"N, 52°21'57"W)

Area 2 is a 500 by 700 m well developed slump located 500 m west of the Karrat 2017 rock avalanche at 950-1200 m elevation (Fig. 1B, 2C). The area could not be visited during fieldwork due to the steepness of the terrain and the near

265 constant rock falls (Fig. 2E). Drone inspection of the 50 m high back scarp showed that bedrock is exposed there (Fig. 2D) demonstrating that bedrock could be involved in the slumping. The area appears as a bulge in the oldest ArcticDEM strip (3 June 2008) indicating that activity in the area could be older than this. However, it is not possible to identify the onset of activity using either Landsat or older aerial images due to their coarse spatial and temporal resolution. Bessette-Kirton et al. (2017) calls the area the West landslide and suggests movement to have started between 13 May 2015 and

270 16 May 2016 based on WorldView imagery. This is in accordance with InSAR analysis showing the first subtle signs of



deformation in the area as a loss of coherence during 3 May 2015 and 15 May 2015. We interpret a ML 1.8 seismic event on 13 May 2015 at 17:14Z (table 2) from the area to represent the exact time of the initiation. Deformation of the outer boundary of the area is clearly visible in all InSAR images from end of May 2015 with movement on the order of 1 mm/day (Fig. 4A). After September 2015 and up to the present day the entire area shows loss of coherence in InSAR which can be due to fast motion or change in surface properties, both of which indicating ongoing activity (Fig. 4B-D). This is in agreement with the very broken up fabric observed in optical satellite images (Fig. 3) and in the field (Fig. 2C, D), indicating both fast movement and change of surface properties. Assuming that the height of the back scarp represents the minimum average thickness of the unstable mass, we tentatively model the volume of Area 2 to be at least $13 \times 10^6 \text{ m}^3$ (by multiplying the area of $260\,000 \text{ m}^2$ by an average thickness 50 m). Paris et al. (2019) used volumes between 2×10^6 and $38 \times 10^6 \text{ m}^3$ for the area for tsunami modelling mentioning that the $38 \times 10^6 \text{ m}^3$ is the more realistic estimate.

Area 3 ($71^\circ 38' 32'' \text{N}$, $52^\circ 21' 23'' \text{W}$)

Area 3 is an 800 by 500 m area located between the scarp of the Karrat 2017 rock avalanche and Area 2 (Fig 1B, 2C). A clear backscarp is not visible but the area shows signs of deformation since May 2015 (coinciding with the initiation of Area 2) and decorrelation over the entire area in all interferograms since 21 June 2017 (the first acquisition after the 17 June 2017 rock avalanche) (Fig. 4A-D). Localized rock falls are seen in Sentinel-2 images and during the field visit (Fig. 2E). It has an overall hummocky surface in recent ArcticDEM strips and a broken up internal fabric was observed (Fig. 2G) indicating significant internal strain. Upslope the area seems to be defined by the western continuation of the backscarp of the Karrat 2017 rock avalanche and it is reasonable to assume that it is sliding on the same basal sliding plane. This area is described here for the first time. We infer activity in Area 3 to have started in May 2015 and increased considerably after 17 June 2017 as the block dislocated in the Karrat 2017 rock avalanche would have supported the area and prevented it from moving. The volume is constrained by using the western continuation of the back scarp and the basal sliding plane of the Karrat 2017 rock avalanche. The western extent of the area is confined by the observed movement in InSAR. This gives a tentative volume of $11 \times 10^6 \text{ m}^3$.

Other activity in the Karrat Landslide Complex area

Several seismic events have been tied to activity in the Karrat Landslide Complex occurring both before and after the Karrat 2017 rock avalanche. Svennevig et al. (2019) describes a seismic event from the 26 Marts 2018 and suggested it was related to activity in the landslide area based on observed rockfall in Sentinel-2 images before and after the event. Several seismic events during the period from 2009 and to the time of submission are suspected to be associated with landslide activity and are listed chronologically in table 2. Another example is the ML 1.9 non-tectonic seismic event that occurred on 1 June 2017 at 20:55Z in the area, with an S-P phase arrival time difference at the seismic station NUUG corresponding to the distance between Nuugaatsiaq and the Karrat Landslide Complex area. The seismic signal is similar to those of the Karrat 2009, 2016 and 2017 rock avalanches (Fig. 5f). The event could not be confirmed by InSAR and optical interpretation due to poor data coverage in the short period between the event and the later Karrat 2017 rock avalanche. It is thus reported here as a seismic event that is possibly a landslide.

The events up until the time of submission are listed in table 2.



Summary table 2: Chronological listing of events at the Karrat Landslide Complex

Interpreted event (see text)	Time	Note	Evidence/data source			
			Seismic (ML)	Optical	DEM	DInSAR
Area 1 initiates	Pre-1953	Observed in legacy GEUS aerial images (1953), Active sub-areas today (DInSAR)		X		X
Karrat 2009 rock avalanche	2009-09-01T14:09Z	First recent (historical) activity and landslide.	2.7	X	X	
Seismic event	2014-09-19T04:30Z	Similar signal to later seismic events	2.0			
Area 2 and 3 initiates	2015-05-13T17:14Z	Deformation only in parts of area 3, localised deformation in area of 2017 avalanche source	1.8		X	X
Karrat 2016 rock avalanche	2016-11-15T11:34Z	Second historical landslide	2.1	X	X	X
Seismic event /landslide?	2017-06-01T20:55Z	The seismic signal is interpreted to be a landslide but this is not resolved by the other datasets	1.9			
Karrat 2017 rock avalanche	2017-06-17T23:39Z	Described by Bessette-Kirton et al. (2017) and Gauthier et al. (2018) and eye witnesses	4.2	X	X	X
Seismic event	2018-02-21T01:10Z		1.7			
Seismic event	2018-03-26T21:21Z	Described by Svennevig et al. (2019)	1.9	X		
Seismic event	2018-04-19T20:18Z	Several consecutive seismic events over a period of two hours	1.9			
Seismic event	2018-08-13T10:04Z	Movement several places in the Karrat Landslide Complex including large parts of Area 2	1.2	X	X	X
Seismic event	2018-08-17T01:15Z and 01:18Z	Interpreted to possibly be a landslide from seismic signature, but this is not resolved by the other datasets	1.7			
Seismic event	2019-10-08T01:50Z	Interpreted to possibly be a landslide from seismic signature, but this is not resolved by the other datasets	0.9			

Discussion

310 Evaluation of the workflow

This study shows the effectiveness of combining complementary remote sensing techniques to establish precise time and location of a long series of landslide activity. It is an inexpensive setup relying on freely available and continuously updated datasets. Although much can be accomplished without fieldwork, the multidisciplinary approach cannot stand alone: It is an effective tool for identifying and investigating active landslide areas, but actual field validation is necessary

315 in order to further assess the risk.

Evolution of the Karrat Landslide Complex

As our compilation of results from the multi-disciplinary approach show, the Karrat 2017 rock avalanche was not an isolated event, but part of an ongoing process of landslide erosion focused in the Karrat Landslide Complex, (Fig 1A and Fig. 6B). This erosion can be subdivided into one or several earlier phases and a series of recent events since 2009.

320

Previous activity

Area 1 was active well before 1953 (the time of the oldest aerial photograph of the area) as shown by the well-developed backscarp and a hummocky morphology indicating significant internal strain (Fig. 2A). Whether the area was active or dormant at this point in time is unclear. Field observations from east of the Karrat 2009 rock avalanche shows that prehistoric rock avalanche deposits are present east of the historic landslides. The individual back scarps and lobes of these are not readily identified indicating that they are very old. A 0.10 km² lobe shaped boulder field below the area of

325



the future scarp of the Karrat 2017 rock avalanche could furthermore be interpreted as the lobe of a minor landslide modified as a rock glacier/debris flow (Figs 2A, 3A). The Karrat 2017 rock avalanche has now erased this feature. These observations point to a previous stage of activity in the Karrat Landslide Complex, possibly several 100s or 1000s of years old.

Recent activity

The first confirmed and dated recent landslide in the eastern part of the Karrat Landslide Complex is the Karrat 2009 rock avalanche, with seismic characteristics comparable to other confirmed landslides in the Karrat Landslide Complex. This is the earliest detected seismological event as the first GLISN stations came into operation during the summer of 2009. As the time period from the Karrat 2009 rock avalanche and forward has reasonable satellite and seismological coverage, the hiatus in activity from the Karrat 2009 rock avalanche to the activity on 19 September 2014 is taken as an indication that nothing major occurred in this time interval.

Area 2 starts to be active from May 2015 as seen in InSAR and a seismic event (Fig. 4A). In addition, localised deformation is observed in part of Area 3 and subareas of Area 1. One-and-a-half years later the Karrat 2016 rock avalanche occurred followed by the seismic event (possible landslide) on 1 June 2017 culminating in the main event: the Karrat 2017 rock avalanche. Based on the available data, we cannot conclude whether precursory movement took place before the avalanches in 2016 and 2017, however, interpretation of the optical imagery rules out a long-term development prior to the three avalanches in eastern Karrat, in contrast to Area 1, 2 and 3. The continued activity observed in InSAR demonstrates that Area 2 and 3 near the Karrat 2017 rock avalanche is not at rest, as further exemplified by the ML 1.9 seismic event and associated minor rockfall on 26 March 2018 (Svennevig et al., 2019) along with multiple similar seismic events (Table 2). The absence of seismic events and landslides in the decades before the Karrat 2009 rock avalanche is taken as an indication that the area was relative dormant prior to this time (Fig. 3A).

The east to west migration of the rock avalanches in the eastern part of the Karrat Landslide Complex suggests a westward migration of a fracture acting as back scarps for the three historical landslides. This, along with the ongoing deformation detected by InSAR in Area 2 and 3 (Fig. 4d), points to the area just west of the Karrat 2017 rock avalanche as having the highest risk of future landslides. The relationship of Area 1 to the other parts of the Karrat Landslide Complex is ambiguous. The trend of the bedding (s0 foliation) acting as a dip slope basal surface of rupture of the Karrat 2009, 2016 and 2017 rock avalanches seems to be situated just below sea level to the west below Area 1 and might act as the basal sliding surface of this also (Fig. 1B).

Possible trigger mechanisms

It has not been possible to determine exactly what triggers individual landslides and seismic events in the Karrat area and why there seems to be a recent peak (since 2009). However, the events are distributed throughout all seasons and, from the limited data we have available, no seasonal change in activity can be seen (Fig. 6C). This indicates that something with longer period than the seasonal cycle could be at work.



365 We hypothesize that the slope instability is induced by permafrost degradation (Draebing et al., 2014; Krautblatter et al.,
2013). The regional air temperature has increased by 4-5 °C since 1880 and has been accelerating since c. 1990 (Cappelen
et al., 2018). The prehistoric activity in the complex described here could have taken place during a previous climatic
optimums such as the Holocene optimum where climatic conditions in the arctic are thought to be similar to those of
today (Axford et al., 2019). The subsequent slow cooling could have stabilized the slopes again until the recent warming.
370 With the projected temperature increase of up to 8 °C towards 2100 (IPCC, 2013) a range of landslide risk factors is
expected to increase, including permafrost degradation and thusly the risk of landslides from the Karrat Landslide
Complex could be expected to increase.

A variety of methods could be applied to test this hypothesis such as dating pre-historic (Holocene) landslide activity,
375 analysing aerial images from the past century to constrain historic evolution (creep) and installing climate sensors to
constrain the present permafrost conditions of the slope. Bathymetrical studies of the seabed just of the Karrat Landslide
Complex could also be included.

Regional hazard evaluation and context

380 As a whole, landslide intensity in the Karrat area (geological area of Proterozoic metasediments interfolded with Archean
gneiss: Fig. 1) is not particularly higher than elsewhere in Greenland (Svennevig, 2019). In this context, the Karrat
Landslide Complex is a local entity and an outlier with respect to landslide intensity as neighbouring slopes in the fjord
system with similar types of bedrock show no abnormal landslide activity. This indicates that local conditions on the
slope are responsible for the high intensity such as s0 parallel dipslope weaknesses and subvertical fracture systems (Fig.
385 2F) along with possible permafrost degradation. The regional landslide hazard in the Karrat area, with the exception of
the Karrat Landslide Complex, is thus not considered to be higher than elsewhere in Greenland.

A consequence of the multistage evolution of the Karrat Landslide Complex is that Gauthier et al. (2018) and Paris et al.
(2019) overestimated the volume of the Karrat 2017 rock avalanche. Gauthier et al. (2018) using an ArcticDEM strip
390 from May 2015 and Paris et al. (2019) using a Spot6 stereoscopic image acquired on 22 July 2013 both estimated 45 x
10⁶ m³ of material effectively reached the sea. Both of these estimates include DEMs from before the Karrat 2016 rock
avalanche, and thus include this volume in their estimate of the total volume that failed on 17 June 2017. Thus the tsunami
run-up estimates by Paris et al. (2019) using the overestimated volumes may be taken as minimum estimates as the
volumes used to train the tsunami model was overestimated. Bessette-Kirton et al. (2017) uses a DEM from satellite
395 images collected on 6 May 2017 and thus do not include the volume of the 2016 rock avalanche in their volume estimate
of minimum 33.4 x 10⁶ m³. A detailed evaluation of volumes of the Karrat 2017 rock avalanche based on oblique photos
from before and after the 2017 landslide is under way (Sørensen et al in prepXX).

Seismological signature of a landslide

400 From the analysis in this paper we have built an experience database of the seismic signature of landslides. It is not an
easy task to separate the signals of a landslide from other sources of shaking – mainly cryogenic seismic events. We have



analysed events from the Karrat area, using both the location of events, the seismic signature and the evidence from optical and InSAR satellite data to distinguish the types of events. The tectonic events are easy to separate from the non-tectonic events (including landslides) (Fig. 5) based on the frequency content and clear P wave arrival. The seismic signal from the major Karrat 2017 rock avalanche is also clearly not a tectonic event – there is no P wave arrival and only a very low frequency S arrival. However, the cryogenic seismic events and smaller landslide events have many characteristics in common. They have a longer duration, a lower frequency content, and often no or very unclear P arrivals. (Fig. 5 I & J). The geographical observation that several large outlet glaciers are found in the area around the Karrat landslide area makes it necessary to look deeper into the characteristics of these non-tectonic events. We have looked at the time difference between P and S arrivals at the Nuugaatsiaq seismic station (when possible). This time difference can be translated into a distance using an earth model with the P and S wave velocities. If the distance from Nuugaatsiaq matched the distance to the Karrat area, it is an indication that it might be a landslide. However, there are several large outlet glaciers within 30 – 60 km of Nuugaatsiaq, and with the uncertainty in location up to 50 km, the time difference is not a conclusive parameter. We have also looked at the duration of the events. Typically, the cryogenic seismic events have a duration of several minutes, while the known and suspected landslide events are shorter – from 45 s to 90 s. But there are also suspected cryogenic seismic events that are of the same duration as suspected landslide events. Currently, we must rely on supporting evidence from the satellite data in order to confirm or dismiss a suspected landslide event seen seismically.

A denser local seismograph network in central West Greenland has been rolled out during the summer of 2019. This will improve the location accuracy of events in the area – including the Karrat Landslide Complex – allowing event location to help separate non-tectonic events into cryogenic seismic events and potential landslide events.

Conclusions and outlook

This study shows the effectiveness of using the multi-disciplinary setup described in Svennevig et al. (2019) for studying landslides in remote Arctic areas. We show that the disastrous Karrat 2017 rock avalanche was not a single event. Smaller landslide events have taken place in the years preceding the major event and continue to do so. The recent landslides took place in 2009, 2016 and 2017 and an increasing number of small events occurred from 2014 onwards. There is also evidence of prehistoric activity in the Karrat Landslide Complex. The Karrat Landslide Complex continues to be very active after the Karrat 2017 rock avalanche and specifically three areas of continued activity named Area 1, 2 and 3 may pose a future hazard. A consequence of resolving the multistage evolution of the Karrat Landslide Complex is that previous studies (Gauthier et al., 2018; Paris et al., 2019) have overestimated the volume of the catastrophic avalanche. The volume of material entering the fjord is an important input to tsunami models and will have implications for estimating the range of the generated wave and ultimately for the risk assessment related to future landslides from the areas with continued activity.

The consequence of a tsunami from a “worst case” landslide from the Karrat Landslide Complex to the two abandoned villages of Nuugaatsiaq and Illorsuit should be addressed.



The distribution of the events over the annual cycle indicates that there is no seasonal signal for what triggered landslides and events. We hypothesize that the slope instability is caused by permafrost degradation. However, further work on this is required in order to confirm this.

440 As our observations all are after the individual events, we obviously cannot forecast coming events. But we have learned that being alert to smaller events in a known landslide area is crucial for the mitigation of the risk of large, tsunamigenic landslides. Additionally, by establishing the seismic, InSAR, and optical signatures of precursors or landslides, it is possible to be alerted of new possible events, both in the Karrat area and elsewhere in isolated arctic areas.

445 Although our multi-disciplinary setup has proved to be successful in describing the evolution of the Karrat Landslide Complex, the present study also provides insight to areas of future development: The upgrade of the seismological network in West Greenland in summer 2019 will improve the accuracy of the location of recorded events and thus relatively cheaply improve our understanding of landslide events in the area by helping distinguishing between cryogenic seismic and landslide events. However, further work is needed to be able to better differentiate between the signals generated by glacier flow and landslide activity. An important lesson from using our current setup is that the workflow
450 would be significantly improved if InSAR analysis and the inspection of optical satellite imagery were conducted routinely, facilitating the search for correlations with the seismic data -and vice versa. This is important for quickly assessing and understanding the scope in the case of a future landslide event.

Data availability

455 All Greenland seismological data are freely available at GEOFON data centre of the GFZ German Research Centre for Geosciences and IRIS Data Services. Sentinel 1 and 2 data are available through the European Earth Observation "Copernicus" program. Landsat Images are available through the USGS Earthexplorer.

Author contributions

460 The manuscript was written by Kristian Svennevig with significant contributions from Trine Dahl-Jensen and Marie Keiding. Kristian Svennevig carried out interpretation of optical data and data integration. John Peter Merryman Boncori, Sara Salehi, Anne M. Solgaard and Marie Keiding carried out processing and interpretation of Sentinel-1 data and wrote the method section on this. Trine Dahl-Jensen wrote the method section on seismology. Trine Dahl-Jensen, Tine B. Larsen and Peter H. Voss carried out processing and interpretation of seismic data and on this. All authors reviewed and approved
465 the manuscript.

Acknowledgements

The governments of Denmark and Greenland funded the "Screening analyses of the risk for serious landslides in Greenland" in 2018 for which the original technical work was undertaken. The facilities of IRIS Data Services, and



470 specifically the IRIS Data Management Center are funded through the Seismological Facilities for the Advancement of
Geoscience and EarthScope (SAGE) Proposal of the National Science Foundation under Cooperative Agreement EAR-
1261681. We acknowledge the European Union Copernicus Program and ESA for the use of Sentinel-1 and 2 data.
Landsat images courtesy of the U.S. Geological Survey. The paper is published under permission of GEUS. Seismological
data collected in the Disco Bay under the INTAROS project was used in the landslide screening. INTAROS has received
475 funding from the European Union's Horizon 2020 research and innovation programme under grant agreement No 727890.
Professor John R Hopper is thanked for constructive comments to this manuscript.

References

- Axford, Y., Lasher, G. E., Kelly, M. A., Osterberg, E. C., Landis, J., Schellinger, G. C., Pfeiffer, A., Thompson, E. and
480 Francis, D. R.: Holocene temperature history of northwest Greenland – With new ice cap constraints and chironomid
assemblages from Deltasø, *Quat. Sci. Rev.*, 215, 160–172, doi:10.1016/J.QUASCIREV.2019.05.011, 2019.
- Besette-Kirton, E., Allstadt, K., Pursley, J. and Godt, J.: Preliminary Analysis of Satellite Imagery and Seismic
Observations of the Nuugaatsiaq Landslide and Tsunami, Greenland, [online] Available from:
[https://www.usgs.gov/natural-hazards/landslide-hazards/science/preliminary-analysis-satellite-imagery-and-seismic?qt-](https://www.usgs.gov/natural-hazards/landslide-hazards/science/preliminary-analysis-satellite-imagery-and-seismic?qt-science_center_objects=0#qt-science_center_objects)
485 [science_center_objects=0#qt-science_center_objects](https://www.usgs.gov/natural-hazards/landslide-hazards/science/preliminary-analysis-satellite-imagery-and-seismic?qt-science_center_objects=0#qt-science_center_objects) (Accessed 6 November 2017), 2017.
- Cappelen, J., Vinther, B. M., Kern-Hansen, C., Laursen, E. V. and Jørgensen, P. V.: Greenland - DMI Historical
Climate Data Collection 1784-2017. [online] Available from: [http://www.dmi.dk/laer-om/generelt/dmi-](http://www.dmi.dk/laer-om/generelt/dmi-publikationer/Url:http://www.dmi.dk/laer-om/generelt/dmi-publikationer/Website:www.dmi.dk)
[publikationer/Url:http://www.dmi.dk/laer-om/generelt/dmi-publikationer/Website:www.dmi.dk](http://www.dmi.dk/laer-om/generelt/dmi-publikationer/Website:www.dmi.dk), 2018.
- Carlà, T., Intrieri, E., Raspini, F., Bardi, F., Farina, P., Ferretti, A., Colombo, D., Novali, F. and Casagli, N.:
490 Perspectives on the prediction of catastrophic slope failures from satellite InSAR, *Sci. Rep.*, 9(1), 1–9, 2019.
- Chao, W. A., Wu, T. R., Ma, K. F., Kuo, Y. T., Wu, Y. M., Zhao, L., Chung, M. J., Wu, H. and Tsai, Y. L.: The large
Greenland landslide of 2017: Was a Tsunami warning possible?, *Seismol. Res. Lett.*, 89(4), 1335–1344,
doi:10.1785/0220170160, 2018.
- Clinton, J., Larsen, T., Dahl-Jensen, T., Voss, P. and Nettles, M.: Special event: Nuugaatsiaq Greenland landslide and
495 tsunami, *Inc. Res. Institutions Seismol. Washington, DC* [online] Available from:
<https://ds.iris.edu/ds/nodes/dmc/specialevents/2017/06/22/nuugaatsiaq-greenland-landslide-and-tsunami/>, 2017.
- Clinton, J. F., Nettles, M., Walter, F., Anderson, K., Dahl-Jensen, T., Giardini, D., Govoni, A., Hanka, W., Lasocki, S.,
Lee, W. S., McCormack, D., Mykkeltveit, S., Stutzmann, E. and Tsuboi, S.: Seismic Network in Greenland Monitors
Earth and Ice System, *Eos, Trans. Am. Geophys. Union*, 95(2), 13–14, doi:10.1002/2014EO020001, 2014.
- 500 Dahl-Jensen, T., Larsen, T. B., Woelbern, I., Bach, T., Hanka, W., Kind, R., Gregersen, S., Mosegaard, K., Voss, P. and
Gudmundsson, O.: Depth to Moho in Greenland: receiver-function analysis suggests two Proterozoic blocks in
Greenland, *Earth Planet. Sci. Lett.*, 205(3–4), 379–393, doi:10.1016/S0012-821X(02)01080-4, 2003.
- Dahl-Jensen, T., Larsen, L. M., Pedersen, S. A. S., Pedersen, J., Jepsen, H. F., Pedersen, G. K., Nielsen, T., Pedersen,
A. K., Von Platen-Hallermund, F. and Weng, W. L.: Landslide and tsunami 21 November 2000 in Paatuut, West
505 Greenland, *Nat. Hazards*, 31(1), 277–287, doi:10.1023/B:NHAZ.0000020264.70048.95, 2004.
- Draebing, D., Krautblatter, M. and Dikau, R.: Interaction of thermal and mechanical processes in steep permafrost rock



- walls: A conceptual approach, *Geomorphology*, 226, 226–235, doi:10.1016/J.GEOMORPH.2014.08.009, 2014.
- Ekström, G., Nettles, M. and Abers, G. A.: Glacial Earthquakes, *Science* (80-.), 302(5645), 622 LP – 624, doi:10.1126/science.1088057, 2003.
- 510 Gauthier, D., Anderson, S. A., Fritz, H. M. and Giachetti, T.: Karrat Fjord (Greenland) tsunamigenic landslide of 17 June 2017: initial 3D observations, *Landslides*, 15(2), 327–332, doi:10.1007/s10346-017-0926-4, 2018.
- Henderson, G. and Pulvertaft, T. C. R.: The stratigraphy and structures of the Precambrian rocks of the Umanak area, West Greenland, *Meddelelser Dansk Geol. Foren.*, 17, 1–20, 1967.
- Henriksen, N., Higgins, A. K., Kalsbeek, F. and Pulvertaft, T. C. R.: Greenland from Archaean to Quaternary
- 515 Descriptive text to the 1995 Geological map of Greenland, 1:2 500 000. 2nd edition, *Geol. Surv. Denmark Greenl. Bull.*, 18, 126, 2009.
- Hovikoski, J., Pedersen, G. K., Alsen, P., Lauridsen, B. W., Svennevig, K., Nøhr-hansen, H., Sheldon, E., Dybkjær, K., Bojesen-Koefoed, J. A., Piasecki, S., Bjerager, M. and Ineson, J.: The Jurassic–Cretaceous lithostratigraphy of Kilen, Kronprins Christian Land, eastern North Greenland, *Bull. Geol. Soc. Denmark*, 66, 61–112, 2018.
- 520 IPCC: Climate Change 2013: The Physical Science Basis. Contribution of Working Group I to the Fifth Assessment Report of the Intergovernmental Panel on Climate Change., 2013.
- Krautblatter, M., Funk, D. and Günzel, F. K.: Why permafrost rocks become unstable: a rock–ice-mechanical model in time and space, *Earth Surf. Process. Landforms*, 38(8), 876–887, doi:10.1002/esp.3374, 2013.
- Mott, A. V., Bird, D. K., Grove, M., Rose, N., Bernstein, S., Mackay, H. and Krebs, J.: Karrat Isfjord: A newly
- 525 discovered Paleoproterozoic carbonatite-sourced REE deposit, central West Greenland, *Econ. Geol.*, 108(6), 1471–1488, doi:10.2113/econgeo.108.6.1471, 2013.
- Nettles, M., Larsen, T. B., Elósegui, P., Hamilton, G. S., Stearns, L. A., Ahlstrøm, A. P., Davis, J. L., Andersen, M. L., de Juan, J., Khan, S. A., Stenseng, L., Ekström, G. and Forsberg, R.: Step-wise changes in glacier flow speed coincide with calving and glacial earthquakes at Helheim Glacier, Greenland, *Geophys. Res. Lett.*, 35(24), doi:10.1029/2008GL036127, 2008.
- 530 Paris, A., Okal, E. A., Guérin, C., Heinrich, P., Schindelé, F. and Hébert, H.: Numerical Modeling of the June 17, 2017 Landslide and Tsunami Events in Karrat Fjord, West Greenland, *Pure Appl. Geophys.*, 176(7), 3035–3057, doi:10.1007/s00024-019-02123-5, 2019.
- Pedersen, S. A. S., Larsen, L. M., Dahl-jensen, T., Jepsen, H. F., Krarup, G., Nielsen, T., Pedersen, A. K., Von Platen-
- 535 Hallermund, F. and Weng, W. L.: Tsunami-generating rock fall and landslide on the south coast of Nuussuaq , central West Greenland, *Geol. Greenl. Surv. Bull.*, 191, 73–83 [online] Available from: <http://www.geus.dk/publications/review-greenland-01/gsb191p73-83.pdf>, 2002.
- Podolskiy, E. A. and Walter, F.: Cryoseismology, *Rev. Geophys.*, 54(4), 708–758, 2016.
- Poli, P.: Creep and slip: Seismic precursors to the Nuugaatsiaq landslide (Greenland), *Geophys. Res. Lett.*, 44(17), 8832–8836, doi:10.1002/2017GL075039, 2017.
- 540 Porter, C., Morin, P., Howat, I., Noh, M.-J., Bates, B., Peterman, K., Keesey, S., Schlenk, M., Gardiner, J., Tomko, K., Willis, M., Kelleher, C., Cloutier, M., Husby, E., Foga, S., Nakamura, H., Platson, M., Wethington, M. J., Williamson, C., Bauer, G., Enos, J., Arnold, G., Kramer, W., Becker, P., Doshi, A., D’Souza, C., Cummens, P., Laurier, F. and Bojesen, M.: ArcticDEM, Harvard Dataverse [online] Available from: <https://doi.org/10.7910/DVN/OHHUKH>, 2018.
- 545 Rosen, P. A., Hensley, S., Joughin, I. R., Li, F. K., Madsen, S. N., Rodriguez, E. and Goldstein, R.: Synthetic aperture



radar interferometry, Proc. IEEE, 88, 333–382, doi:https://doi.org/10.1109/5.838084, 2000.

Sørensen, E. V. and Guarnieri, P.: Remote geological mapping using 3D photogrammetry: an example from Karrat, West Greenland, Geol. Surv. Denmark Greenl. Bull., 41, 63–66, 2018.

Svennevig, K.: Preliminary landslide mapping in Greenland, Geol. Surv. Denmark Greenl. Bull., 43(June),
550 e2019430207, doi:10.34194/geusb-201943-02-07, 2019.

Svennevig, K., Solgaard, A. M., Salehi, S., Dahl-Jensen, T., Merryman Boncori, J. P., Larsen, T. B. and Voss, P. H.: A multidisciplinary approach to landslide monitoring in the Arctic: Case study of the March 2018 ML 1.9 seismic event near the Karrat 2017 landslide, Geol. Surv. Denmark Greenl. Bull., 43(June 2017), e2019430208, doi:10.34194/geusb-201943-02-08, 2019.

555 Westergaard-Nielsen, A., Karami, M., Hansen, B. U., Westermann, S. and Elberling, B.: Contrasting temperature trends across the ice-free part of Greenland, Sci. Rep., 8(1), 1–6, doi:10.1038/s41598-018-19992-w, 2018.

Figures

Figure 1:

560 A: Simplified geological map of the region based on Henriksen et al. (2009) showing nearby seismic stations (NUUG and UMMG), prehistoric landslides (Svennevig, 2019) and the area of Fig. 1B. B: The Karrat Landslide Complex shown on a Sentinel-2 rgb image from 20 April 2019 where the coastal slope has a light snow cover emphasising the landslides and structures. Transparent polygons are the three rock avalanches (2009, 2016, and 2017) and the three active areas (1, 2, and 3). The stippled lines at the rock avalanches is the extent of the individual scarps. Notice the recent rockfall from
565 Area 2 (dark stria south of the area). Positions of field photos in Fig. 2 are shown.

Figure 2:

A: 1953 1:45 000 scale aerial photograph of the Karrat landslide Complex showing the well-developed state of the active area; Area 1. The three stippled lines to the east shows the positions of the scarps of the future rock avalanches (colours match Fig. 1B). Notice also the lobate morphology (X) and boulder field (Y) indicating pre historic landslide activity. B-G Field photos from the Karrat Landslide Complex in the summer of 2019. B: Oblique helicopter photo of Area 1. From the shore to the top of the backscarp is 1000 m and the backscarp is up top 120 m high for scale. C: Oblique helicopter photo of Area 2 and 3 and the three rock avalanches (2009, 2016, 2017). Notice the hummocky morphology of Area 2 and 3 and the dust cloud east of area 3. Area 2 is 1200 m across for scale. D: UAV photo of the backscarp of Area 2. The
575 arrow points to where bedrock is exposed indicating that the slide is not a superficial feature. E: Field photo from 1 km west of Area 2 showing the bulging active area (arrow) and near constant rockfalls from Area 2, 3 and the 2017 backscarp producing a dust cloud also visible in C. View is towards the east. F: Field photo of the bedrock geology of the coastal slope 1.5 km west of Area 1. View is towards the west. Sub vertical jointing and S0 foliation dipping 20-30° towards the fjord are prominent. The geologist is standing next to a vertical open fracture with a small normal offset apparent on the
580 surface that could be a model for the development of the backscarp of the rock avalanches. Photo by Simon Mose Thaarup.



G: UAV photo of the backscarp of the Karrat 2017 rock avalanche looking towards the NW. The mottled interior of Area 3 is apparent along with the bulging nature of Area 2 in the background. See Fig. 1b for locations.

Figure 3

585 Optical satellite images of the eastern part of the Karrat Landslide Complex, the locus of recent rock avalanches. A: Scene
from 1 May 2009 before the historical landslides initiated, a presumed ancient landslide deposit (lobe) is marked with X
(from ©Google Earth, image credit: Maxar Technologies). B: Sentinel-2 image from 5 April 2016 showing the situation
after the Karrat 2009 rock avalanche of 1 September 2009 at 14:09Z. C: Sentinel-2 image from 1 March 2017 showing
the situation after the Karrat 2016 rock avalanche of 11 November 2016 at 14:09Z. D: Sentinel-2 image from 10 April
590 2018 showing the situation after the Karrat 2017 rock avalanche of 17 June 2017 at 23:39Z.

Figure 4

Single-pass interferograms of the eastern part of the Karrat landslide Complex. A: Ascending track 90 during 26 June –
8 July 2015. The deformation in the broader part of Area 1 is not clearly seen in this viewing geometry, however, two
595 subareas with decorrelation due to high deformation rates are apparent. Deformation in Area 2 and 3 and below the 2017
rock avalanche is visible, but the steep slope itself is in layover due to the geometry of the satellite acquisition. B:
Ascending track 90 during 12-24 September 2015. Area 2 shows decorrelation indicating acceleration of deformation
rates. C: Ascending track 90 during 11-17 November 2016, spanning the 2016 rock avalanche, which shows up as
completely decorrelated. D: Descending track 25 during 20 July – 11 August 2018, a year after the 2017 rock avalanche.
600 The area of the 2017 avalanche shows partly coherent and incoherent deformation. Area 2 and 3 both show complete
decorrelation due to high deformation rates. The upper right part of the interferograms shows varying coherent fringes
and decorrelation due to rapid movements of ice glaciers.

Figure 5

605 Seismic signatures of major events. All figures show the unfiltered data of the vertical component from the seismic station
at Nuugaatsiaq (NUUG). A) is a 5 min extract of the Karrat 2017 landslide. B) - H) are 1 min 10 sec extracts for different
types of events, all at similar distances from NUUG. B) is a tectonic earthquake (EQ), clearly distinguishable by higher
frequencies. C) is a cryogenic seismic event, here the full length of the signal is not represented in the 1 min 10 sec extract.
D) and E) are known landslides (Karrat 2016 and Karrat 2017), and F) – H) are interpreted as possible landslides in the
610 Karrat area, but this is not supported by the other datasets. The glacial and landslide/possible landslide events are clearly
different to the tectonic EQ, but the differences between the glacial and landslide events are subtle. I) and J) are 10 min
data extracts from possible landslide events and a cryogenic seismic event. The cryogenic seismic events last several
minutes, while the minor possible landslide events last under two minutes.



615 **Figure 6**

A: Data coverage, B: timeline of historic events in the Karrat Landside Complex and C: yearly distribution of landslides and seismic events.

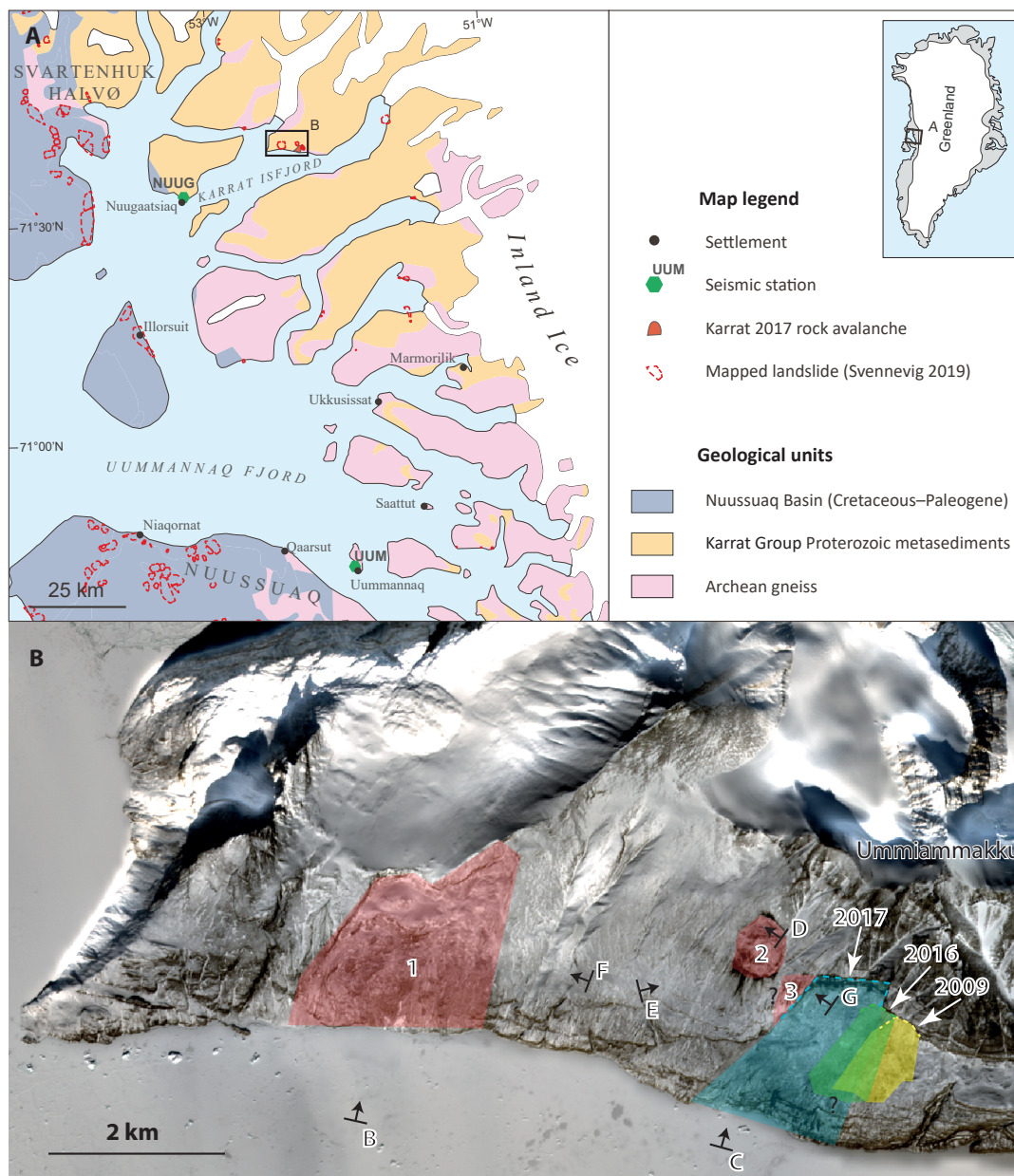


Fig. 1

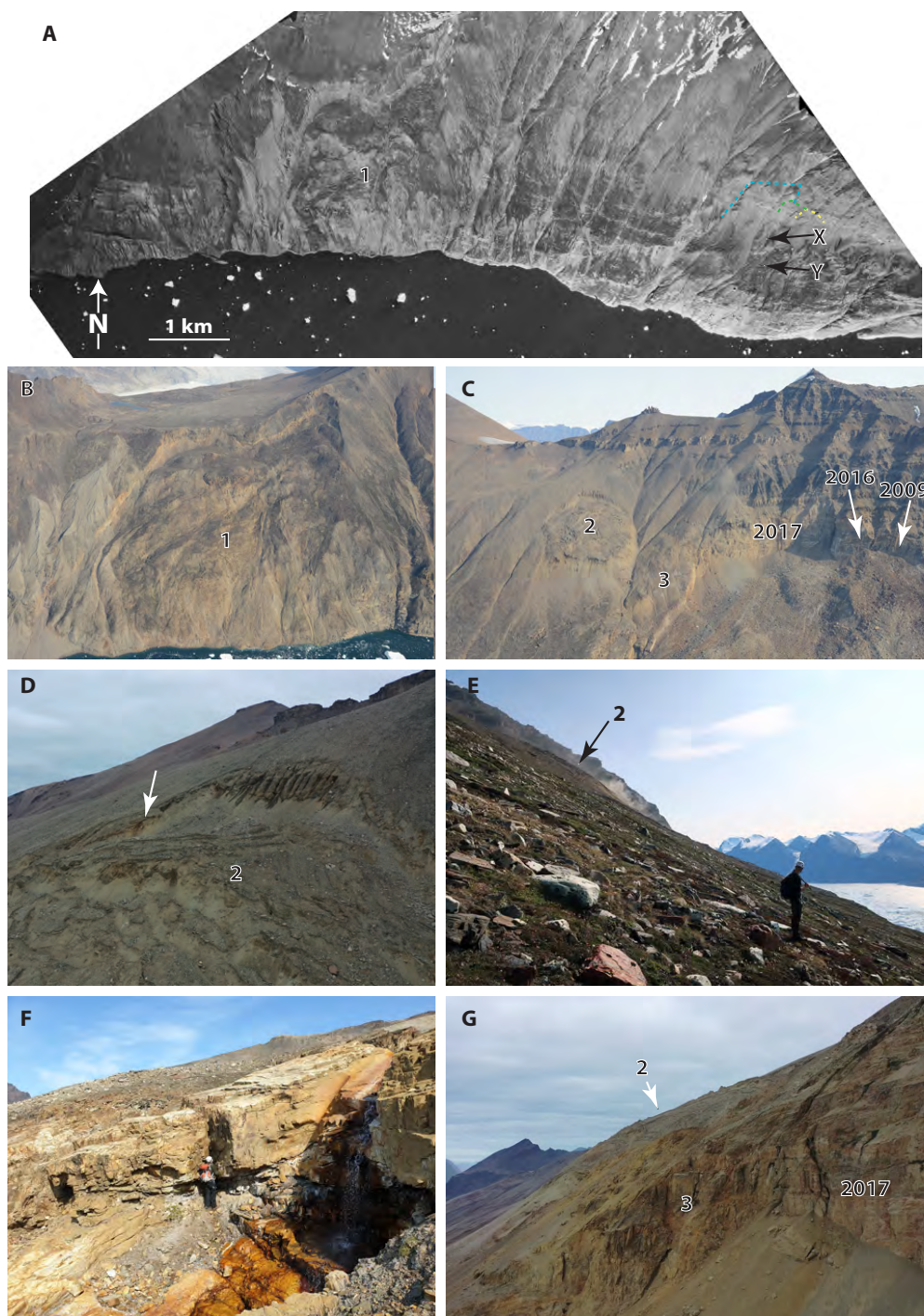
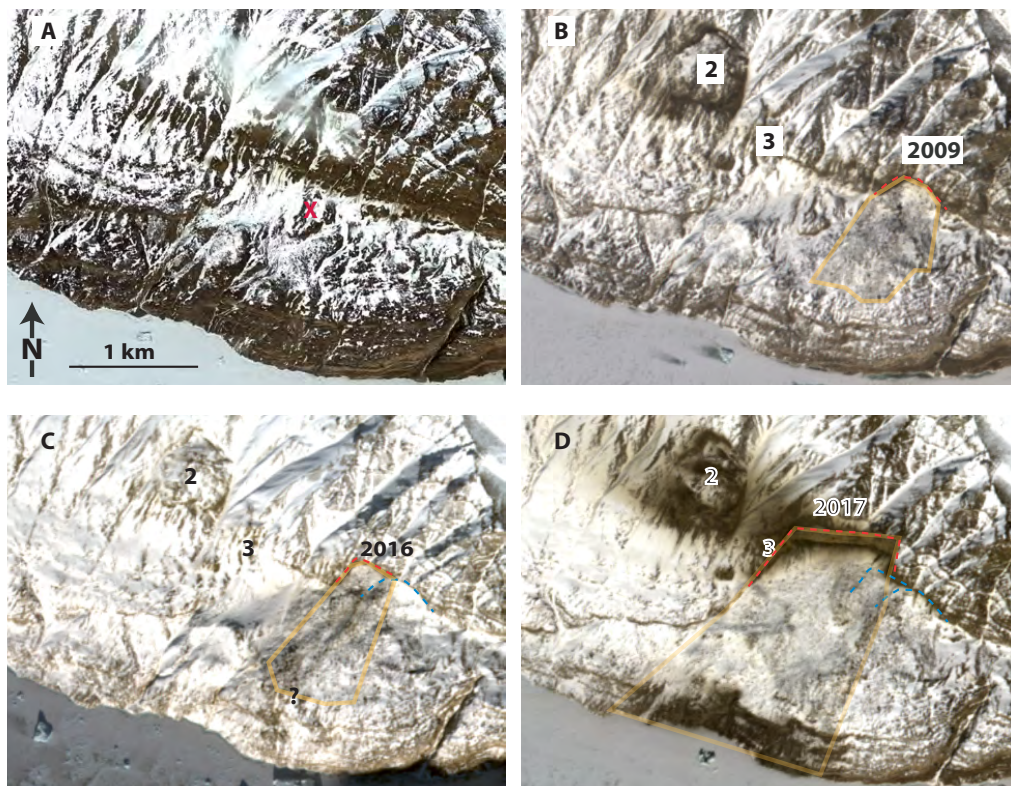


Fig. 2



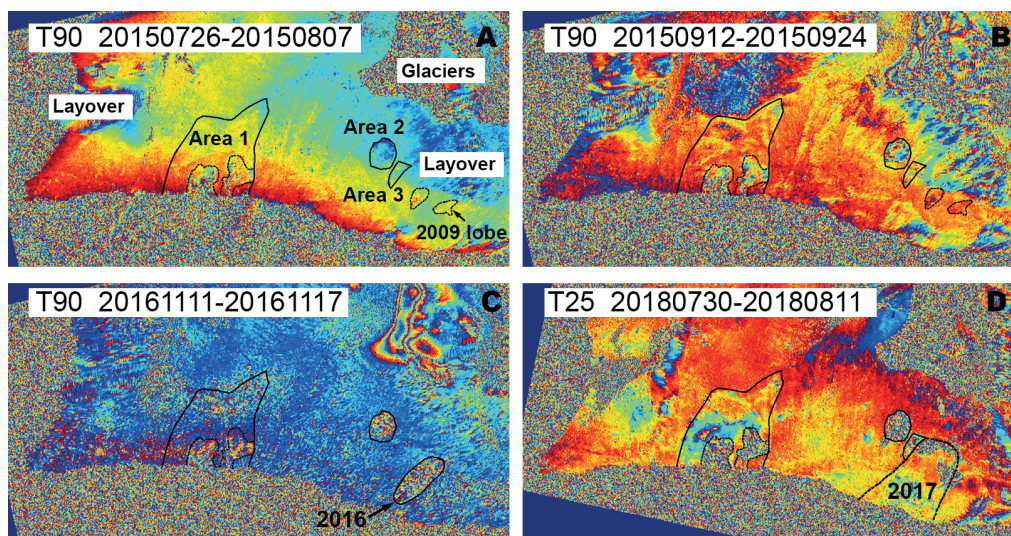


Fig. 4

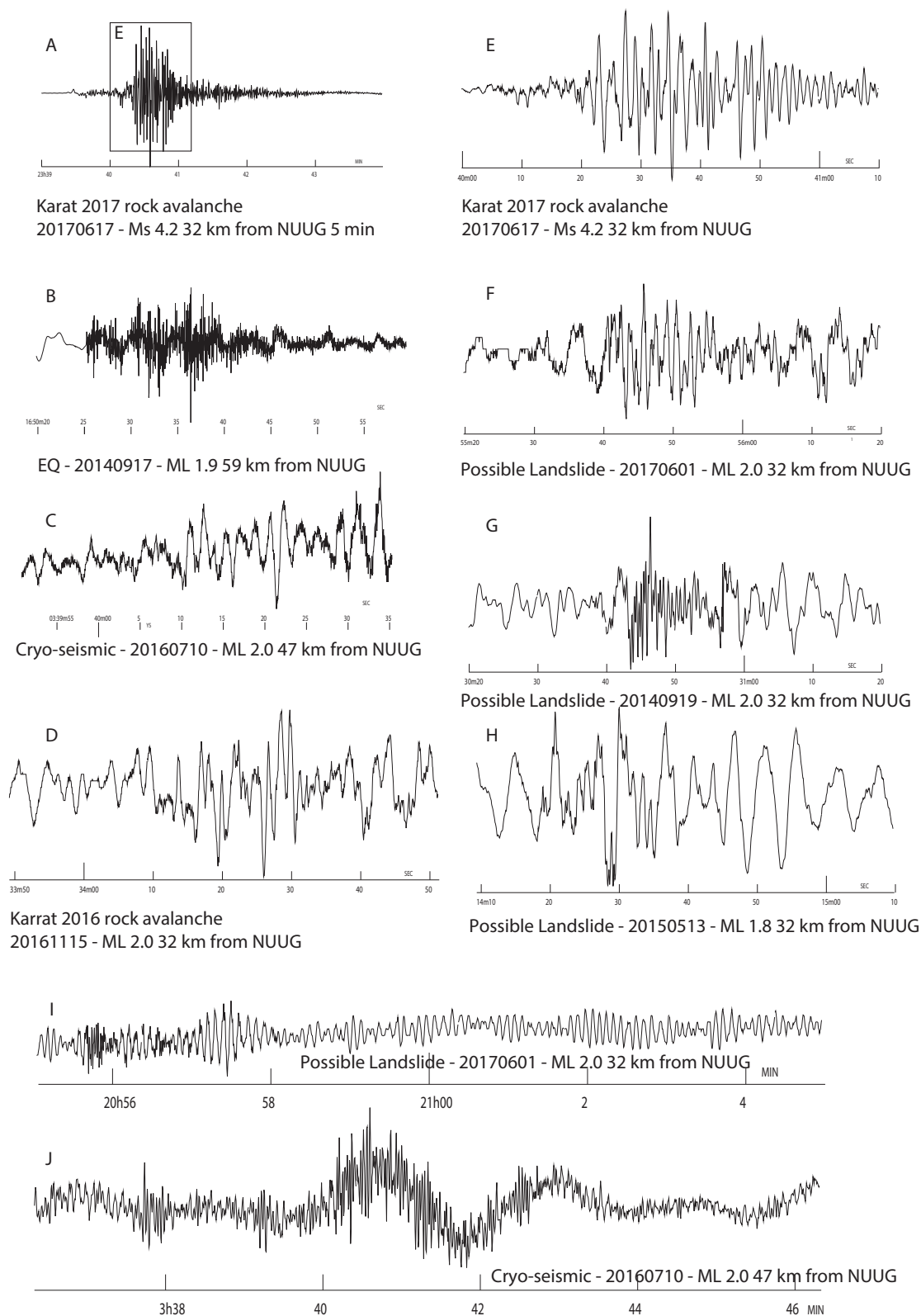


Fig. 5

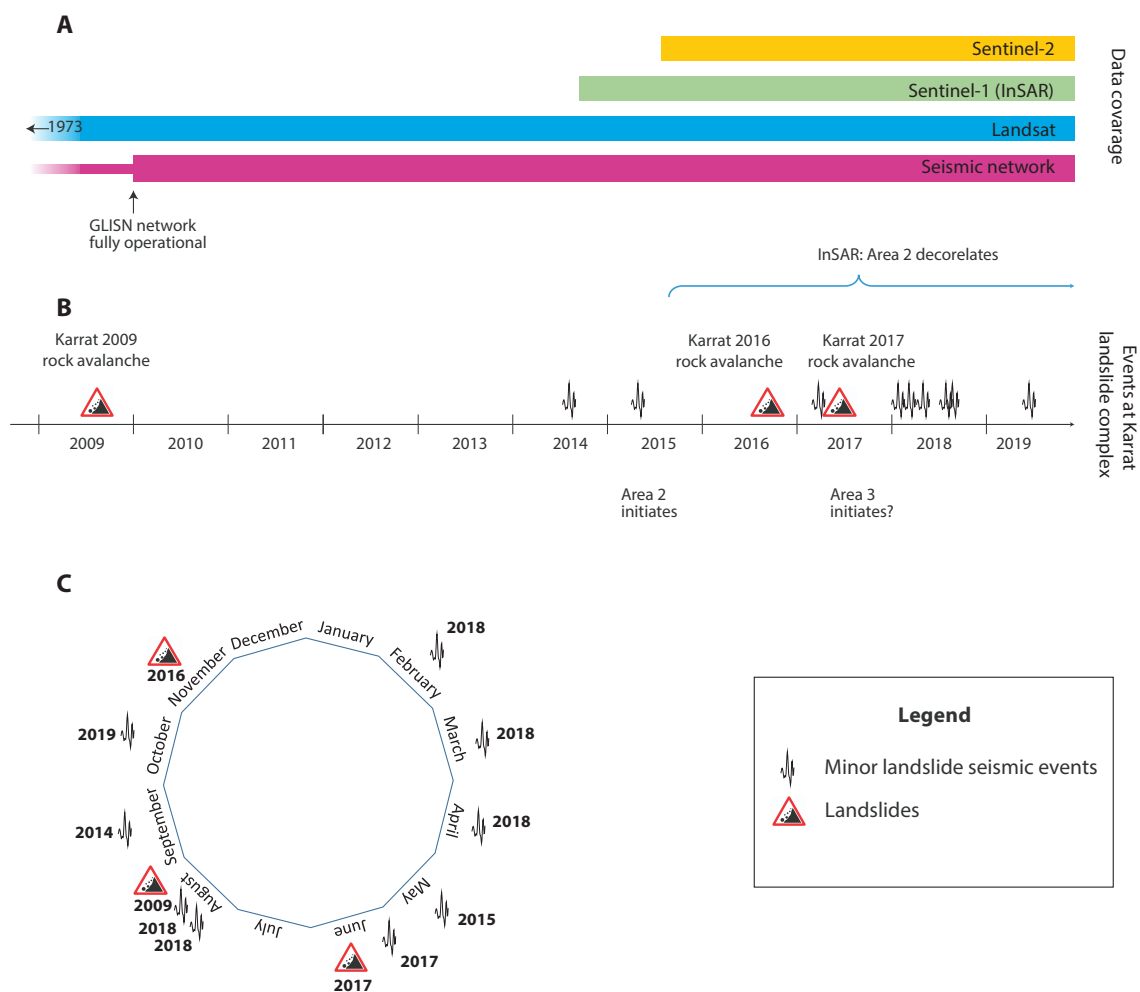


Fig. 6